Theoretical Study of the Geometric and Electronic Structures and Spectra of *trans*-$ME_2(PH_3)_4$ Complexes (M = Mo, W; E = S, Se, Te)

Woo-Sung Kim and Nikolas Kaltsoyannis*,†

Centre for Theoretical and Computational Chemistry, University College London, 20 Gordon Street, London WC1H 0AJ, England

Received May 30, 1997

The optimized geometries of $ME_2(PH_3)_4$ complexes (M = Mo, W; E = S, Se, Te) have been calculated using nonlocal, quasi-relativistic density functional theory. In all cases the most stable structure was found to have C_{4v} symmetry. Comparison with crystallographic data (D_{2d} symmetry) for $ME_2(PMe_3)_4$ (M = Mo, E = S, Se, Te; M = W, E = Se, Te) reveals excellent agreement between theory and experiment. The ground-state electronic structures of all six title complexes are found to resemble those obtained from previous local density functional (Xα) calculations and hence to differ from *ab initio* molecular orbital schemes that place the metal d_{xy}-localized level several electronvolts below the chalcogen p_π lone pair highest occupied molecular orbital. Electronic transition energies are calculated using the transition state method. A consistent assignment of the electronic absorption spectra of $WE_2(PMe_3)_4$ and $MoE_2(Ph_2PCH_2CH_2PPh_2)_2$ (E = S, Se, Te) is proposed. This assignment is different from either the experimental or *ab initio* conclusions, though on the key question of the origin of the lowest energy band the present density functional data reinforce previous *ab initio* conclusions that it is due to a chalcogen $p_\pi \rightarrow \pi^*$ promotion and not the anticipated ligand field transition. Thus the density functional and *ab initio* approaches agree when used to calculate physically observable electronic promotion energies, although their ground-state molecular orbital orderings differ considerably.

Introduction

There is currently a great deal of interest in the synthesis, characterization, reactivity, and electronic structure of compounds of the general formula *trans*-ME_2L_4 (M = Mo, W; E = O, S, Se, Te; L = phosphine).[1−8] These molecules have pseudo-octahedral geometries, in which the two trans chalcogen atoms are doubly bonded to the d^2 M(IV) center. Parkin and co-workers have reported the synthesis and crystallographic characterization of $MoE_2(PMe_3)_4$ (E = S, Se, Te)[7] and $WE_2(PMe_3)_4$ (E = Se, Te),[3,6] while Cotton and Feng indicate the imminent publication of similar data for $MoE_2(L\text{-}L)_2$ (E = O, S, Se, Te; L-L = dppee ($Ph_2PCH_2CH_2PPh_2$)).[8] The electronic structures of these systems have been studied by both experimental[4,7,8] and theoretical techniques.[5,8] The electronic absorption spectra of $WE_2(PMe_3)_4$ (E = S, Se, Te) were reported by Thorp and co-workers,[4] while Cotton and Feng discuss those of $MoE_2(dppee)_2$ (E = S, Se, Te).[8] Murphy and Parkin report the wavelength of the most intense absorption in the spectra of $MoE_2(PMe_3)_4$ (E = S, Se, Te).[7] The electronic structures of $WE_2(PH_3)_4$ (E = O, S, Se, Te) were investigated computationally by Kaltsoyannis,[5] using the discrete variational Xα (DV-Xα) implementation of density functional theory (DFT). Very recently, Cotton and Feng reported *ab initio* studies of the ground-state electronic structure and electronic absorption spectra of $MoE_2(PH_3)_4$ (E = O, S, Se, Te).[8]

Until Cotton and Feng's contribution, the ground-state electronic structures and assignments of the electronic absorption spectra seemed clear enough. The DV-Xα calculations on $WE_2(PH_3)_4$[5] supported the view that their valence electronic structures could be rationalized on the basis of an axially compressed ligand field,[9] with the two metal-localized electrons occupying the d_{xy}-based highest occupied molecular orbital (HOMO). The electronic absorption spectra were also interpreted on the basis of this MO model. The *ab initio* results of Cotton and Feng, however, call this whole approach into question, suggesting not only that the HOMO of these molecules is actually a chalcogen p_π lone pair orbital but also that the first peak in the electronic absorption spectra is not the previously accepted ligand field $d_{xy} \rightarrow \pi^*$ transition but is instead a chalcogen $p_\pi \rightarrow \pi^*$ promotion.

In this contribution we report the results of nonlocal, quasi-relativistic density functional calculations of the geometric and electronic structures and transition energies of $ME_2(PH_3)_4$ (M = Mo, W; E = S, Se, Te). Our aim is 2-fold, the resolution of the discrepancy between the previous theoretical methods and a consistent assignment of the electronic absorption spectra of $WE_2(PMe_3)_4$ and $MoE_2(dppee)_2$.

Computational Details

All calculations were performed with the Amsterdam Density Functional program suite.[10,11] Triple-ζ Slater-type orbital valence basis sets were employed for Mo, W, and Te (ADF type IV). The basis sets

† Fax: +44 171 380 7463. E-mail: n.kaltsoyannis@ucl.ac.uk.

(1) Brewer, J. C.; Thorp, H. H.; Slagle, K. M.; Brudvig, G. W.; Gray, H. B. *J. Am. Chem. Soc.* **1991**, *113*, 3171.
(2) Rabinovich, D.; Parkin, G. *J. Am. Chem. Soc.* **1991**, *113*, 9421.
(3) Rabinovich, D.; Parkin, G. *J. Am. Chem. Soc.* **1991**, *113*, 5904.
(4) Paradis, J. A.; Wertz, D. W.; Thorp, H. H. *J. Am. Chem. Soc.* **1993**, *115*, 5308.
(5) Kaltsoyannis, N. *J. Chem. Soc., Dalton Trans.* **1994**, 1391.
(6) Rabinovich, D.; Parkin, G. *Inorg. Chem.* **1994**, *33*, 2313.
(7) Murphy, V. J.; Parkin, G. *J. Am. Chem. Soc.* **1995**, *117*, 3522.
(8) Cotton, F. A.; Feng, X. *Inorg. Chem.* **1996**, *35*, 4921.
(9) Ballhausen, C. J.; Gray, H. B. *Inorg. Chem.* **1962**, *1*, 111.
(10) te Velde, G.; Baerends, E. J. *J. Comput. Phys.* **1992**, *99*, 84.
(11) *ADF⟨2.2⟩*; Department of Theoretical Chemistry, Vrije Universiteit: Amsterdam, 1997.

S0020-1669(97)00651-4 CCC: $15.00
Published on Web 02/05/1998

Table 1. Selected Bond Lengths (Å) and Angles (deg) for $MoE_2(PH_3)_4$ (E = S, Se, Te)

	$MoS_2(PH_3)_4$		$MoSe_2(PH_3)_4$		$MoTe_2(PH_3)_4$	
	calc (C_{4v})	exptl[a] ($D2_d$)	calc (C_{4v})	exptl[a] (D_{2d})	calc (C_{4v})	exptl[a] (D_{2d})
			Bond Lengths			
Mo−E′	2.299	2.254	2.425	2.383	2.683	2.597
Mo−E″	2.256	2.254	2.391	2.383	2.626	2.597
Mo−P	2.508	2.517	2.508	2.519	2.501	2.522
P−H′	1.427		1.428		1.428	
P−H″	1.428		1.431		2.418	
			Bond Angles			
P−Mo−E′	87.3	82.7	87.8	82.6	86.7	82.0
P−Mo−E″	92.7	97.2	92.2	96.9	93.3	98.0

[a] Data for $MoE_2(PMe_3)_4$ from ref 7.

Table 2. Selected Bond Lengths (Å) and Angles (deg) for $WE_2(PH_3)_4$ (E = S, Se, Te)

		$WSe_2(PH_3)_4$		$WTe_2(PH_3)_4$	
	$WS_2(PH_3)_4$ calc (C_{4v})	calc (C_{4v})	exptl[a] (D_{2d})	calc (C_{4v})	exptl[b] (D_{2d})
		Bond Lengths			
W−E′	2.333	2.466		2.725	2.596
W−E″	2.280	2.416	2.380	2.644	2.596
W−P	2.257	2.523		2.513	2.508
P−H′	1.429	1.429		1.43	
P−H″	1.429	1.428		1.43	
		Bond Angles			
P−W−E′	86.6	86.7		86.1	82.1
P−W−E″	93.4	93.3		93.9	97.9

[a] Data for $WSe_2(PMe_3)_4$ from ref 6. [b] Data for $WTe_2(PMe_3)_4$ from ref 2.

for S, Se, P, and H were also triple-ζ, supplemented by two polarization functions (one d and one f, ADF type V). Quasi-relativistic scalar frozen cores were used for all elements, P (2p), S (2p), Se (3d), Te (4d), Mo (4p), and W(5p). Relativistic core potentials were computed using the ADF auxiliary program "Dirac". The local density functional of Vosko, Wilk, and Nusair was employed,[12] together with the nonlocal exchange and correlation corrections due to Perdew and Wang.[13] All molecular geometries were fully optimized and confirmed as true energy minima by the observation of only positive eigenvalues in the Hessian matrixes.

Electronic transition energies were computed using the transition state method.[14,15] Separate calculations were converged for each transition.

Results and Discussion

A. Geometric Structures. Calculated bond lengths and angles for all six of the title complexes are given in Tables 1 and 2, together with the experimental data available for $ME_2(PMe_3)_4$ (M = Mo, W; E = S, Se, Te). The first point to note is that, while the X-ray structures of $MoE_2(PMe_3)_4$ (E = S, Se, Te) and $WE_2(PMe_3)_4$ (E = Se, Te) indicate D_{2d} molecular symmetry, all of our calculated data are for C_{4v} structures. All attempts to optimize the geometries in D_{2d} symmetry led to molecules with at least one imaginary vibrational frequency (i.e. they were not true minimum structures) and total molecular binding energies slightly less negative than when C_{4v} symmetry was specified. Furthermore, the vibrational frequencies generated from the C_{4v} structures were all real.

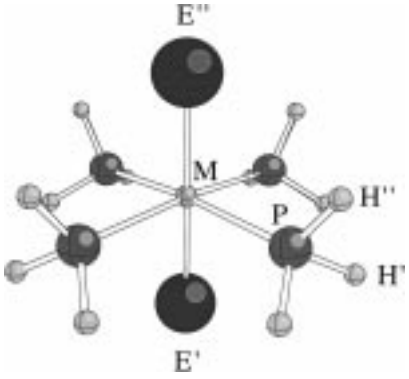

Figure 1. Ball-and-stick representation of a generalized $ME_2(PH_3)_4$ molecule with C_{4v} symmetry.

A ball-and-stick representation of a generalized C_{4v} $ME_2(PH_3)_4$ molecule is shown in Figure 1. Tables 1 and 2 reveal that the agreement between the calculated and experimental metal−chalcogen and metal−phosphorus bond lengths is extremely good. The latter are all within 0.02 Å of the experimental value, and the *greatest* discrepancy between the calculated metal−nearer chalcogen distance (M−E″) and the experimental bond length is 0.048 Å (for M = W; E = Te). It should be noted, however, that the C_{4v} calculations yield two metal−chalcogen distances while a D_{2d} geometry implies only one, and the longer metal−chalcogen distance (M−E′) is further from the experimental value than the M−E″. Nevertheless we feel that our calculated bond lengths are more than satisfactory given the size of the molecules under investigation.

Comparison of the calculated and experimental P−M−E angles is less informative given that the C_{4v} geometry has all four P atoms nearer to E′ than E″, whereas the D_{2d} arrangement places two P atoms closer to E′ than E″ and two nearer to E″. This, together with the replacement of Me groups by H in the calculated structures, provides a plausible explanation of the ca. 5° differences between the calculated and experimental P−M−E angles.

The principal aim of this work is not to compare experimental and theoretical geometries but to study electronic structures and transition energies. The geometries chosen for the electronic investigations were in all cases the calculated C_{4v} structures detailed in Tables 1 and 2. We believe that this lends our study an internal consistency not present if we employ crystallographically determined structural parameters and that any discrepancies should in any case be small given the agreement between the theoretical and experimental molecular geometries.

B. Ground-State Electronic Structures. Part 1. As mentioned in the Introduction, DFT and *ab initio* calculations differ considerably in their prediction of the ground-state orbital ordering of $ME_2(PH_3)_4$. Both DV-Xα[5] (M = W; E = S, Te) and SW-Xα[8] (M = Mo; E = S) DFT support the orbital ordering expected from an axially compressed pseudo-octahedral ligand field around the metal center.[9] Thus the HOMO is largely composed of the metal−ligand nonbonding metal d_{xy} atomic orbital (which in a genuinely octahedral molecule forms part of the t_{2g} set of orbitals), and the lowest unoccupied MO (LUMO) is a degenerate pair of metal−chalcogen π antibonding orbitals primarily composed of the metal d_{xz} and d_{yz} AOs (the remaining t_{2g} MOs in O_h symmetry). *Ab initio* calculations on $MoE_2(PH_3)_4$ (E = S, Se, Te),[8] however, predict that the HOMO is actually a chalcogen lone pair orbital; the d_{xy}-based MO is significantly more stable than the HOMO (by several electronvolts) in all three molecules. Although the same orbitals are occupied in both the DFT and *ab initio* MO schemes (and hence

(12) Vosko, S. H.; Wilk, L.; Nusair, M. *Can. J. Phys.* **1980**, *58*, 1200.
(13) Perdew, J. P.; Chevary, J. A.; Vosko, S. H.; Jackson, K. A.; Pederson, M. R.; Singh, D. J.; Fiolhais, C. *Phys. Rev. B* **1992**, *46*, 6671.
(14) Slater, J. C. *Adv. Quantum Chem.* **1972**, *6*, 1.
(15) Slater, J. C. *The Calculation of Molecular Orbitals*; Wiley: New York, 1979.

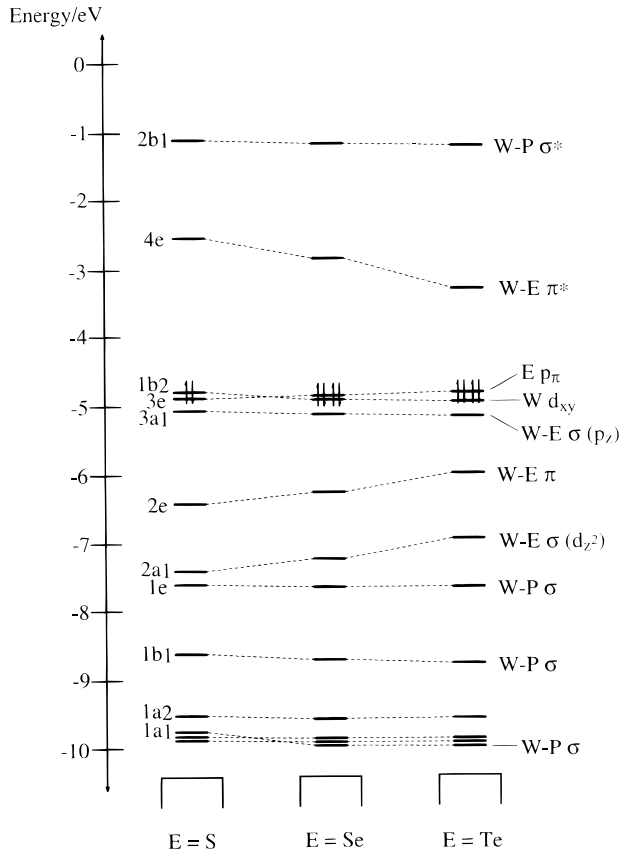

Figure 2. Density functional ground-state molecular orbital energy level diagram of the valence orbitals of $WE_2(PH_3)_4$ (E = S, Se, Te). The highest occupied orbital is the $1b_2$ for $WS_2(PH_3)_4$ and the 3e for $WSe_2(PH_3)_4$ and $WTe_2(PH_3)_4$.

both methods agree that $ME_2(PH_3)_4$ have closed-shell singlet ground states) the discrepancy in the orbital ordering is quite dramatic.

We therefore decided to reinvestigate $ME_2(PH_3)_4$ using more sophisticated density functional methods than the previous Xα studies. The principal improvements were the use of the parametrization of Vosko, Wilk, and Nusair[12] instead of the Xα functional, supplemented by a variety of nonlocal (gradient) exchange and correlation corrections. Superior basis sets were also employed. In this paper we report the results of calculations conducted with the gradient corrections due to Perdew and Wang,[13] as we have been impressed with the ability of this approach to reproduce the properties (e.g. ground-state geometries, ionization energies) of a wide variety of molecules, but it should be noted that the use of several of the other nonlocal methods advocated in the literature did not significantly alter the MO ordering obtained. This is presented for $WE_2(PH_3)_4$ (E = S, Se, Te) in Figure 2, from which it may be seen that the more sophisticated DFT calculations essentially reinforce the Xα approach.

The $1a_1$, $1b_1$, and 1e MOs are primarily associated with W−P σ bonding. The $2a_1$ and $3a_1$ orbitals are chalcogen p_z-based (in phase and out of phase, respectively), with smaller contributions from the W d_{z^2} ($2a_1$) and p_z ($3a_1$) AOs. The 2e MO is π bonding between the W d_{xz} and d_{yz} AOs and the p_x and p_y orbitals of the chalcogens. By contrast, the 3e MO is almost exclusively chalcogen p_π in character—this is the HOMO of the *ab initio* calculations.[8] Finally among the occupied MOs comes the W d_{xy}-based $1b_2$ level. This orbital, which contains the two metal d-localized electrons of the formally W(IV) complexes, is the HOMO of $WS_2(PH_3)_4$ and the next HOMO of $WSe_2(PH_3)_4$ and $WTe_2(PH_3)_4$, a very different result from the *ab initio* study which placed this MO 3−4 eV more stable than the chalcogen p_π lone pair HOMO. The LUMO of all three compounds is the 4e W−E π* orbital that, together with the $1b_2$ orbital, is related to the t_{2g} orbitals of a purely octahedral compound. The last MO shown in Figure 2 is the $2b_1$ metal $d_{x^2-y^2}$-based W−P σ* orbital.

Table 3. Electronic Transition Energies (nm) for $WE_2(PH_3)_4$ (E = S, Se, Te)

		$WS_2(PH_3)_4$		$WSe_2(PH_3)_4$		$WTe_2(PH_3)_4$	
transition	transition type	calc (DFT)	exptl[a]	calc (DFT)	exptl[a]	calc (DFT)	exptl[a]
3e → 4e	$p_\pi \rightarrow \pi^*$	503	552	583	621	768	752
$1b_2$ → 4e	$d_{xy} \rightarrow \pi^*$	482	476	524	526	630	671
$3a_1$ → 4e	$p_z \rightarrow \pi^*$	448	405	497	452	595	549
$1b_2$ → $2b_1$	$d_{xy} \rightarrow d_{x^2-y^2}$	331		327		323	
2e → 4e	$\pi \rightarrow \pi^*$	317	341	361	375	458	442

[a] Data for $WE_2(PMe_3)_4$ from ref 4.

Clearly, then, the DFT and *ab initio* approaches differ as to the ground-state valence orbital ordering of the title complexes. Although at first sight this may appear unsatisfactory, we must bear in mind the physical significance of ground-state eigenvalues obtained via these calculational methods. Koopmans' theorem,[16,17] of course, tells us that the negative of the one-electron energies calculated by the Hartree−Fock (HF) method are the ionization energies of the electrons. Thus the HF MO schemes presented by Cotton and Feng would provide a starting point for the assignment of the photoelectron spectra of $WE_2(PR_3)_4$, were they available (ignoring the well-documented failings of Koopmans' theorem in photoelectron spectroscopy[18]). Ground-state density functional eigenvalues, however, have no corresponding physical significance.[19] Their link with physical observables such as ionization energies and electronic transition energies has been pointed out by Slater[14,15] and involves the calculation of eigenvalues for orbitals with half-electron occupation. As ground state and so-called "transition state" density functional eigenvalue orderings are often significantly different from one another, we should not be unduly alarmed at the differences between the DFT and *ab initio* ground-state orbital orderings. Better to use both methods to calculate some physical observable and then make a comparison. It is to this, in the form of electronic transition energies, that we now turn.

C. Electronic Transitions. The calculated electronic transition energies for $WE_2(PH_3)_4$ (E = S, Se, Te) and the experimental data obtained by Thorp and co-workers for $WE_2(PMe_3)_4$ (E = S, Se, Te)[4] are given in Table 3. All of the theoretical data are taken from DFT calculations in which the two MOs given in the first column of Table 3 have an occupancy corresponding to the removal of half an electron from the lower orbital and its placement in the upper orbital. The transition energy is then obtained as the eigenvalue difference between the two fractionally occupied MOs. All of the calculated transitions are spin-allowed, i.e., the excess α spin over β spin density is constrained to be zero in all calculations. This corresponds to singlet → singlet transitions from the $^1A_1$ (in C_{4v}) molecular ground state. No formally singlet → triplet transition state calculations are possible within ADF. It should be noted that, in the transitions between MOs of e symmetry,

(16) Koopmans, T. *Physica* **1934**, *1*, 104.
(17) Lowe, J. P. *Quantum Chemistry*; Academic Press: New York, 1978.
(18) Eland, J. H. D. *Photoelectron Spectroscopy*; Butterworth: London, 1984.
(19) Parr, R. G.; Yang, W. *Density-Functional Theory of Atoms and Molecules*; OUP: Oxford, U.K., 1989.

Table 4. Electronic Transition Energies (nm) for $MoE_2(PH_3)_4$ (E = S, Se, Te)

		$MoS_2(PH_3)$			$MoSe_2(PH_3)_4$				$MoTe_2(PH_3)_4$			
		calc			calc				calc			
transition	transition type	ab initio[a]	DFT[b]	exptl[c]	ab initio[a]	DFT[b]	exptl[c]	calc DFT[d]	ab initio[a]	DFT[b]	exptl[c]	calc (DFT)[d]
$3e \rightarrow 4e$	$p_\pi \rightarrow \pi^*$	547	552	550	701	640	640	569 (^1A_u)	971	849	770	708 (^1A_u)
		530			676			605 (^1B_u)	941			761 (^1B_u)
		471			597			555 (^1A_u)	828			683 (^1A_u)
$1b_2 \rightarrow 4e$	$d_{xy} \rightarrow \pi^*$	432	508	425	499	551	585	582 ($^1B_{3g}$)	609	659	625	712 ($^1B_{3g}$)
		431		415	498			578 ($^1B_{2g}$)	608			701 ($^1B_{2g}$)
$3a_1 \rightarrow 4e$	$p_z \rightarrow \pi^*$	429	476		481	529	520	496 ($^1B_{2u}$)	565	639		608 ($^1B_{2u}$)
		426			477			495 ($^1B_{3u}$)	559			604 ($^1B_{3u}$)
$1b_2 \rightarrow 2b_1$	$d_{xy} \rightarrow d_{x^2-y^2}$	360	351		373	350		330 ($^1B_{1g}$)	345	347		340 ($^1B_{1g}$)
$2e \rightarrow 4e$	$\pi \rightarrow \pi^*$	279	331	375	350	375	415	353 ($^1B_{1g}$)	468	478	485	442 ($^1B_{1g}$)
		275			339			335 ($^1B_{1g}$)	418			413 ($^1B_{1g}$)
		273			331			352 (^1A_u)	423			479 (^1A_u)

[a] Data (D_{2h} singlet excited states only) from ref 8. [b] Optimized C_{4v} geometry. [c] Data for $MoE_2(dppee)_2$ from ref 8. [d] D_{2h} geometry as employed in ref 8 (excited-state symmetry in parentheses).

it is not possible for us to specify the symmetry of the excited state. For example, while the $d_{xy} \rightarrow d_{x^2-y^2}$ $1b_2 \rightarrow 2b_1$ transition is unambiguously a $^1A_1 \rightarrow {}^1A_2$ promotion, the $3e \rightarrow 4e$ transition gives rise to excited states with spacial symmetries A_1, A_2, B_1, and B_2, of which all bar the A_2 will be singlets.[20,21] We have no way of specifying which excited state we are forming in these cases, and hence it is best to regard our calculated transition energy as an average of the promotions from the molecular ground state to the singlet states possible from the e^3e^1 excited electronic configurations.

The first, and arguably most important, point to note from the data in Table 3 is that the longest wavelength transition is in all cases the $3e \rightarrow 4e$ $p_\pi \rightarrow \pi^*$ promotion. This is in agreement with the *ab initio* studies of $MoE_2(PH_3)_4$[8] and makes a powerful case for a reassignment of the electronic absorption spectra of $WE_2(PMe_3)_4$. The present theoretical data strongly suggest that the lowest energy band is not due to a ligand field transition. This promotion is found to be the second least energetic, and the agreement between theory and experiment for this $d_{xy} \rightarrow \pi^*$ transition (particularly in $WS_2(PH_3)_4$ and $WSe_2(PH_3)_4$) makes the original assignment[4] difficult to defend. It is also noteworthy how, even though the $1b_2$ and $3e$ MOs of $WE_2(PH_3)_4$ have very similar ground-state eigenvalues (Figure 2), the transitions from these orbitals to the 4e LUMO are clearly well separated in energy (and, in the case of $WS_2(PH_3)_4$, reverse the ground-state eigenvalue ordering). This is another example of how unreliable a guide ground-state density functional eigenvalue differences can be when interpreting electronic spectra.

The most intense band in the electronic absorption spectra of $WE_2(PMe_3)_4$ was assigned to a $\pi \rightarrow \pi^*$ transition by Thorp and co-workers.[4] Our data for the $2e \rightarrow 4e$ transition support this assignment, with a pleasing agreement between theory and experiment. The experimental spectra have a fourth band (at 405, 452, and 549 nm, respectively, for $WS_2(PMe_3)_4$, $WSe_2(PMe_3)_4$, and $WTe_2(PMe_3)_4$) that was assigned to the spin-forbidden singlet $\rightarrow$ triplet $\pi \rightarrow \pi^*$ transition. Our data offer the alternative assignment of this band to the $3a_1 \rightarrow 4e$ $p_z \rightarrow \pi^*$ promotion, which has the added appeal of being spin-allowed.

The extinction coefficient of this fourth band in the experimental spectra increases from 600 M^{-1} cm^{-1} in $WS_2(PMe_3)_4$ to 4000 M^{-1} cm^{-1} in $WTe_2(PMe_3)_4$.[4] Unfortunately ADF does not allow us to calculate the intensities of transitions, so we cannot make any direct comparison of the experimental intensity trend with our work. It is interesting, however, to note that the composition of the $3a_1$ MO (see Figure 2 for numbering scheme), which is the p_z orbital from which the electron is promoted in the $p_z \rightarrow \pi^*$ transition, is noticeably different in $WTe_2(PH_3)_4$ in comparison with $WS_2(PH_3)_4$ and $WSe_2(PH_3)_4$. In the latter two molecules this orbital is entirely chalcogen p_z in character, with a negligible contribution from the metal. In $WTe_2(PH_3)_4$, however, there is an 8% W p_z contribution to this MO. Given that the intensity of an electric dipole transition depends upon the difference in dipole moment between the two states between which the electron is moving, it is possible that the different composition of the $3a_1$ MO in $WTe_2(PH_3)_4$ in comparison with the $3a_1$ of $WS_2(PH_3)_4$ and $WSe_2(PH_3)_4$ results in a sufficient change in the electron distribution within the orbital so as to increase significantly the change in dipole moment between the $3a_1$ and 4e levels (p_z and π^* orbitals), thereby increasing the intensity of the transition.

Table 4 presents the calculated electronic transition energies (both DFT and *ab initio*) for $MoE_2(PH_3)_4$ (E = S, Se, Te), together with the experimental data for $MoE_2(dppee)_2$ reported by Cotton and Feng.[8] Our data clearly support the *ab initio* conclusion that the longest wavelength electronic transition in these complexes is also the $p_\pi \rightarrow \pi^*$ promotion and not the ligand field $d_{xy} \rightarrow \pi^*$. The agreement between DFT and experiment for this first transition is remarkable for $MoS_2(PH_3)_4$ and $MoSe_2(PH_3)_4$, though less impressive for $MoTe_2(PH_3)_4$.

The second peak in the spectra of $MoE_2(dppee)_2$ is therefore assigned to the ligand field $d_{xy} \rightarrow \pi^*$ transitions. The agreement between the DFT $d_{xy} \rightarrow \pi^*$ wavelengths and the experimental data is not that good for $MoS_2(PH_3)_4$, though is appreciably better for $MoSe_2(PH_3)_4$ and $MoTe_2(PH_3)_4$. In the experimental spectra of $MoS_2(dppee)_2$ and $MoSe_2(dppee)_2$ there are two peaks in this energy range, though only one in $MoTe_2(dppee)_2$. The peaks in $MoS_2(dppee)_2$ are only 10 nm apart, and hence, the *ab initio* assignment of these to the two states arising from the $d_{xy} \rightarrow \pi^*$ transition in D_{2d} symmetry is entirely plausible. The analogous assignment for $MoSe_2(dppee)_2$, however, is less convincing, for while the *ab initio* calculated states are just 1 nm apart (at 499 and 498 nm) the experimental peaks lie at 585 and 520 nm. We therefore propose an alternative assignment for $MoSe_2(dppee)_2$ in which only the peak at 585 nm is associated with the ligand field transition. That at 520 nm fits much more closely with our calculated $p_z \rightarrow \pi^*$ transition at 529 nm. We should emphasize that this suggestion is based purely

(20) Cotton, F. A. *Chemical Applications of Group Theory;* 3rd ed.; Wiley-Interscience: New York, 1991.
(21) Atkins, P. W.; Child, M. S.; Phillips, C. S. G. *Tables for Group Theory*; OUP: Oxford, U.K., 1970.

on the wavelengths reported by Cotton and Feng; we have not seen the spectra of $MoE_2(dppee)_2$ as they are not yet in the literature.

Cotton and Feng are prevented from adopting this assignment because they have already assigned the $p_z \rightarrow \pi^*$ transitions to the experimental peaks at 375, 415, and 485 nm in $MoS_2(dppee)_2$, $MoSe_2(dppee)_2$, and $MoTe_2(dppee)_2$, respectively. We, however, prefer to free up this $p_z \rightarrow \pi^*$ assignment by equating the experimental peaks at 375, 415, and 485 nm with the $2e \rightarrow 4e$ $\pi \rightarrow \pi^*$ transitions. We believe that, on the basis of matching our theoretical data to the experimental transition wavelengths, our revised assignment is more convincing.[22] For example, the DFT-calculated $\pi \rightarrow \pi^*$ transition for $MoTe_2(PH_3)_4$ comes at 478 nm, only 7 nm away from the experimental peak at 485 nm. Following the suggestion of Cotton and Feng requires us to associate the DFT transition at 639 nm with the experimental value, a difference of 154 nm. Similar, though slightly less dramatic, discrepancies exist for the other two Mo compounds. The *ab initio* data, however, are much less suited to this revised assignment, particularly for $MoS_2(PH_3)_4$. Thus the DFT and *ab initio* calculations differ as to the assignment of these experimental peaks. We feel, however, that our conclusion that they be attributed to the $\pi \rightarrow \pi^*$ transitions is the most appropriate on the basis of our DFT calculations and has the added merit of consistency with the calculated data for $WE_2(PH_3)_4$ (for which there are no *ab initio* studies) and the experimental spectra of $WE_2(PMe_3)_4$. Note that both the $p_z \rightarrow \pi^*$ and $\pi \rightarrow \pi^*$ transitions are spin and dipole allowed in C_{4v}. Hence the fact that the experimental peaks are intense does not favor one of these assignments over the other on selection rule grounds.

The remaining transition, the $1b_2 \rightarrow 2b_1$ ligand field $d_{xy} \rightarrow d_{x^2-y^2}$, has no experimental peak associated with it. Comparison of the *ab initio* and DFT results shows an excellent agreement between the theoretical methods in this case. As noted by Cotton and Feng, the energy of this transition is essentially unaffected by alteration of the chalcogen, the only transition for which this is true.

We turn now to a brief discussion of the data in the fourth columns of the $MoSe_2(PH_3)_4$ and $MoTe_2(PH_3)_4$ sections of Table 4. These transition wavelengths have been calculated using our DFT approach but at the geometries employed by Cotton and Feng,[8] which are based upon the experimentally determined structures of $MoE_2(dppee)_2$ (E = Se, Te), in an attempt to see if the differences between the C_{4v} and D_{2h} geometries result in significantly different calculated transition energies. Although there are a number of points arising from these data, the most important is that, in both cases, the conclusions from our C_{4v} calculations are reinforced at the D_{2h} geometries. For both molecules, the longest wavelength transitions are once again found to be $p_\pi \rightarrow \pi^*$ in origin. In the case of $MoSe_2(PH_3)_4$, the agreement between theory and experiment is worsened on moving from the optimized C_{4v} geometry to the experimentally determined D_{2h}, while for $MoTe_2(PH_3)_4$ the agreement is very much improved. The $d_{xy} \rightarrow \pi^*$ transitions come next in both molecules followed, ca. 100 nm to longer wavelength, by the $p_z \rightarrow \pi^*$. Thus our revised assignment of the experimentally observed 585 and 520 nm transitions of $MoSe_2(dppee)_2$ to the $d_{xy} \rightarrow \pi^*$ and $p_z \rightarrow \pi^*$ promotions, respectively, is supported by our D_{2h} calculations. Furthermore, our assignments of the experimental peaks at 415 and 485 nm for $MoSe_2(dppee)_2$ and $MoTe_2(dppee)_2$ respectively to $\pi \rightarrow \pi^*$ transitions is also supported by the D_{2h} calculations. Finally, it should be noted that the agreement between the C_{4v} and D_{2h} calculations of the ligand field $d_{xy} \rightarrow d_{x^2-y^2}$ transitions is very good for both molecules.

D. Ground-State Electronic Structures. Part 2. The data in Tables 3 and 4 indicate that, even though the DFT and *ab initio* calculations differ in their placement of the metal d_{xy}-based MO in the ground-state electronic structures of the title complexes, they are in much closer agreement over the assignment of the electronic absorption spectra. This result, while reassuring, raises the intriguing question as to which theoretical method provides a more accurate representation of the ground-state electronic structures. Given our earlier discussion of the physical significance of *ab initio* and DFT ground-state eigenvalues, the answer *must* be that we do not know and have no way of telling. Even photoelectron spectroscopy would not establish the ground-state orbital ordering of the neutral molecules, although it might give some useful clues. At the very least it would provide further physical data—ionization energies—against which the two theoretical approaches could be tested. We leave the interested reader to decide for themselves which scheme—Figure 3 of ref 8 or Figure 2 of the present work—most closely reflects the ground-state electronic structures of the title complexes.

Acknowledgment. We thank the Royal Society for an equipment grant, the EPSRC for a grant of CPU time on the "Columbus" central computing facility, and the reviewers for their helpful comments.

IC9706515

(22) It should be noted, however, that the agreement between DFT and experiment for the $e \rightarrow e$ transitions may be somewhat fortuitous, given the e^3e^1 state averaging approximations discussed earlier.